KAPL-P-000177
(K97064)
CONF-9705119--

TPV EFFICIENCY PREDICTIONS AND MEASUREMENTS FOR A CLOSED CAVITY GEOMETRY

C. K. Gethers, C. T. Ballinger, et. al.

May 1997

NOTICE

KAPL ATOMIC POWER LABORATORY SCHENECTADY, NEW YORK 10701

Operated for the U. S. Department of Energy
by KAPL, Inc. a Lockheed Martin company

DISCLAIMER

TPV Efficiency Predictions and Measurements for a Closed Cavity Geometry

C. K. Gethers, C. T. Ballinger, M. A. Postlethwait, D. M. DePoy and P. F. Baldasaro

Lockheed Martin Corporation, Schenectady, New York

Abstract: A thermophotovoltaic (TPV) efficiency measurement, within a closed cavity, is an integrated test which incorporates four fundamental parameters of TPV direct energy conversion. These are: (1) the TPV devices, (2) spectral control, (3) a radiation/photon source, and (4) closed cavity geometry affects. The overall efficiency of the TPV device is controlled by the TPV cell performance, the spectral control characteristics, the radiator temperature and the geometric arrangement. Controlled efficiency measurements and predictions provide valuable feedback on all four. This paper describes and compares two computer codes developed to model 16, 1 cm^2 TPV cells (in a 4x4 configuration) in a cavity geometry. The first code, subdivides the infrared spectrum into several bands and then numerically integrates over the spectrum to provide absorbed heat flux and cell performance predictions (assuming infinite parallel plates). The second, utilizes a Monte Carlo Ray-Tracing code that tracks photons, from birth at the radiation source, until they either escape or are absorbed. Absorption depends upon energy dependent reflection probabilities assigned to every geometrical surface within the cavity The model also has the capability of tallying above and below bandgap absorptions (as a function of location) and can support various radiator temperature profiles. The arrays are fabricated using 0.55 eV InGaAs cells with Si/SiO interference filters for spectral control and at steady state conditions, array efficiency was calculated as the ratio of the load matched power to its absorbed heat flux. Preliminary experimental results are also compared with predictions.

Introduction

In a thermophotovoltaic (TPV) generator, four fundamental systems are integrated to generate useful electrical power from infrared radiation:

- a radiator/photon source
- a semiconductor diode
- a spectral control system/filters
- cavity geometry affects

The primary function of the radiator is to provide infrared energy for TPV conversion. The TPV cell can convert only a fraction of the infrared energy emitted by the radiator into electrical power (typically 28% of the blackbody spectrum for a 1090°C radiator with 0.55 eV TPV cells). Photons with lower energy (below band-

gap photons) contribute to the temperature rise of the cell unless they are reflected back to the radiator. The spectral control system reflects these below bandgap photons back to the radiator and transmits above bandgap photons, which can be converted to electricity by the cell. Also, the system's geometry affects the associated photons, creating polarization, view factor, multiple reflections and angle of incidence concerns that must be accounted for in system models.

By performing controlled efficiency measurements and predictions, valuable feedback can be provided for cell, filter and radiator development. This testing also provides feedback on the integration of these three fundamental systems into a TPV system by incorporating closed cavity geometry effects.

The ability exists for measuring and predicting single cell efficiency using a code that assumes infinite parallel plates. This same quantity can be measured using a calibrated blackbody source and copper block transient calorimetry technique [1]. Excellent agreement was observed between the measured and predicted single cell efficiencies of 0.55 eV indium gallium arsenide (InGaAs) TPV cells which have values of approximately 14% and 13.6±10.0%, respectively. These measurements and predictions correspond to a radiator temperature of ~1090°C and a cell temperature of ~25°C.

The 16 cell (array) efficiency measurements, however, are more complex than those for a single cell. This type of experiment integrates all thermal, electrical and system geometry issues into one measurement. The cavity introduces geometry dependent concerns which include polarization, view factor, multiple reflections, radiator temperature non-uniformities and angle of incidence effects. In addition, there are first order effects such as diode performance, diode matching, illumination uniformity and spectral control that play a role. A substantial amount of work has been performed to quantify these effects through the use of two separate computer codes, an infinite parallel plate code and a Monte Carlo Ray-Tracing code. The first code, TPVCalc, subdivides the infrared spectrum into several bands and then numerically integrates over the spectrum to provide absorbed heat flux and cell performance predictions. The second code, utilizes a Monte Carlo code that tracks photons, from birth at the radiation source, until they either escape the cavity or are absorbed. Absorption depends upon energy dependent reflection probabilities assigned to every geometrical surface within the cavity. The code also has the capability of tallying above and below bandgap absorptions as a function of location, and can support various radiator temperature profiles.

The 16 cell array efficiency, η, is experimentally determined by taking the ratio of the array's maximum power output to its total absorbed radiative heat flux,

$$\eta = \frac{P_{OUT}}{P_{ABS}} = \frac{V_{OC} I_{SC} ff}{\dot{m} C_P \Delta T} \qquad \text{Eqn. 1}$$

where,

P_{OUT} = maximum power output by the array,

P_{ABS} = the array's total absorbed radiative heat flux,

V_{oc} = array open circuit voltage,

I_{sc} = array short circuit current,

ff = array fill factor,

$\dot{m}$ = mass flow rate of the coolant,

C_p = specific heat of coolant and

ΔT = coolant temperature rise between inlet and outlet of the array.

This paper describes and compares two computer codes that were developed to model 16, 1 cm^2 TPV cells (in a 4x4 configuration) in a cavity geometry. Experimental results are also compared with predictions. The arrays are fabricated using 0.55 eV InGaAs cells with Si/SiO interference filters for spectral control.

Experimental Setup

Figure 1 provides a top-down view of the heater cavity with the lid and radiator material removed showing the TPV array below the window. Figure 2 shows a schematic of the heater cavity test stand. The internal walls and window of the heater cavity are polished to minimize photon losses in the wall and to promote uniform illumination incident upon the array. A square 0.08 inch thick piece of high emissivity Poco Graphite functions as the radiator material and rests over the window. The radiator was instrumented with two C-type thermocouples and its surface is approximately 0.300 inches from the surface of the TPV device. The thermocouples have the flexibility of being placed at either the radiator's center or edge.

In all measurements, the radiator was raised to a target temperature and the system allowed to equilibrate (a thermal gradient of ~40°C was measured across the radiator.). After which, the radiative absorbed heat flux and maximum output power of the array were measured and used to calculate array efficiency. All absorbed heat flux measurements were taken with the array in open circuit mode to ensure that the heat flux was transferred to the coolant, and not lost to joule heating of an external load.

Efficiency Predictions - Infinite Parallel Plate Model

The first computer code (TPVCalc) used to model TPV efficiency assumes an infinite parallel flat plate geometry. This model requires radiator temperature as an input and assumes that the radiator is perfectly isothermal. For modeling of the cavity test, an average of the measured edge temperatures was used as the radiator temperature. The code is based on a derivation of the model presented by Baldasaro, *et al* [2], where the efficiency, η, is given by:

$$\eta = F_0 \times \frac{V_{oc}}{E_g} \times \overline{QE} \times ff \times fu_{cell} \times fu_{module} \times f_{unknown} \quad \text{Eqn. 2}$$

where,

F_0 = usable fraction of thermal radiation with energy > E_g,

E_g = cell bandgap energy,

$\overline{QE}$ = average energy weighted charge carrier flux/photon flux of energy > Eg,

fu_{cell} = fraction of total absorbed radiation with energy > E_g,

fu_{module} = fraction of absorbed radiation due to module inactive area,

$f_{unknown}$ = fraction of performance decrement due to non-uniform illumination and cell mismatching effects

Equation 2 is analogous to equation 1 except that it is based on energy ratio parameters. This equation was initially developed to model single cell efficiency and has been modified to account for the additional variables incorporated in 16 cell array efficiency predictions. Specifically, the array equation accounts for fabrication (fu_{module}) and other unknown effects ($f_{unknown}$) such as those caused by illumination and variations in cell matching. Explicit knowledge of the variables in equation 2 is required to accurately predict and measure array efficiency.

In the TPVCalc model, the infrared spectrum is divided into intervals and efficiency is determined by numerically integrating the absorbed heat flux and array output over the spectrum. To calculate the absorbed heat flux in the array, the spectral characteristics of the array and radiator are measured with an Fourier Transform Infrared Spectrometer (FTIR) and numerically integrated to evaluate the spectral utilization of the system. The model also assumes that the only mode of heat transfer is through radiation. This method of calculating absorbed heat flux and array efficiency was compared to the classical grey body solution for radiative exchange between two infinite parallel flat plates. The absorbed heat flux calculated from the model and the heat flux from the classical solutions were identical.

Modeling of the array electrical characteristics is based on measured spectral

quantum efficiency and an analytically determined over-excitation factor, F_o, which is coupled with the spectral characteristics of the radiator and array (Figures 3-5). The fill factor and open circuit voltage of the array is based on the array cell characteristics (bandgap, dark current, series resistance and ideality factor) and the array temperature. The spectral utilization of the module is also dependent on the inactive area of the array which is not present for a single cell.

Monte Carlo Ray-Tracing Code

A Monte Carlo code was also developed to perform photon transport calculations for this specific thermophotovoltaic application. This new Monte Carlo code was used to calculate the heat fluxes, spectral utilization, view factors, and even the photon-induced short circuit current of a 16 cell array of TPV cells. The complex geometric arrangement of the cavity, wavelength dependent photon source and reflection properties make predicting the efficiency of such an arrangement difficult without this multidimensional computer code.

In general, the Monte Carlo method does not solve an explicit transport equation, but rather simulates individual particle histories and records some aspects of their average behavior. The individual probabilistic events that comprise a history are simulated sequentially by sampling physically-based probability distributions that describe the event. A Monte Carlo calculation consists of tracking millions of photon histories from their birth at the source to death at a terminal event (absorption or escape). This data is then tallied by geometric location and post-processed to determine the heat flux absorption and electrical performance of the array.

Assigning Photon Attributes

The Monte Carlo Ray-Tracing code simulates individual photon histories from birth to termination. Location, direction, polarization, and energy of each photon must be determined at birth to completely characterize the individual photons. A temperature distribution across the radiator was measured for the cavity experiments which complicates the Monte Carlo simulation, since the photon production rate and energy spectrum become location dependent due to the temperature distribution. Nevertheless, an analytic description of the photon birth location from the radiator surface can be derived. The number of photons emitted by a blackbody per unit volume, N, is given by [3],

$$N(\vec{r}) = \int_0^\infty n(\vec{r}, E)dE = \frac{8\pi\varepsilon}{(hc)^3}(kT(\vec{r}))^3 \int_0^\infty \frac{\alpha^2 d\alpha}{e^\alpha - 1}. \qquad \text{Eqn. 3}$$

where,

k = Boltzmann's constant,

h = Planck's constant,

ε = radiator emissivity,

c = the speed of light,

$n(\vec{r}, E)dE$ = the blackbody energy spectrum (number of photons of energy dE about E per unit volume per unit energy),

$T(\vec{r})$ = location dependent temperature (K) and

$$\int_0^\infty \frac{\alpha^2 d\alpha}{e^\alpha - 1} \approx 2.4011.$$

A parabolic temperature profile across the radiator is assumed in these calculations based on measured center and edge temperatures. The photon density can be calculated based on the average radiator temperature distribution and converted into a probability distribution describing the photon birth location.

Like the birth location, an analytic solution for the photon directional probability distribution is possible. Integration over solid angles is necessary when calculating a directional probability distribution. Figure 6 shows a schematic representation of solid angle integration where,

$$\int_{4\pi} d\Omega = \int_{\frac{-\pi}{2}}^{\frac{\pi}{2}} \int_0^{2\pi} \sin(\theta) d\phi d\theta = 4\pi. \qquad \text{Eqn. 4}$$

Hence, the average angle for emitted photons from a radiator $\bar{\theta}$ is calculated by integrating over a half space as,

$$\bar{\theta} = \int_0^{\frac{\pi}{2}} \int_0^{2\pi} \theta p(\theta, \phi) \sin(\theta) d\phi d\theta \qquad \text{Eqn. 5}$$

The angular distribution appropriate for a diffuse emitter [4], like graphite, is given by,

$$p(\theta, \phi) = \cos(\theta)/(2\pi), \qquad \text{Eqn. 6}$$

which results in an average angle of 45° from the surface normal. This average angle was used when designing the filters since it is the most probable photon angle of incidence on the filters in the cavity experiments. Notice that the diffuse scattering angle probability distribution (Eqn. 6) is independent of azimuthal angle, ϕ. The azimuthal angle probability distribution is therefore uniformly distributed between 0 and 2π, which is easily sampled in the Monte Carlo Ray-Tracing code by generating a random number, $\xi \in (0, 1)$, and defining,

$$\phi_{sampled} = 2\pi\xi. \qquad \text{Eqn. 7}$$

The scattering angle, θ, can be sampled from the probability distribution given in

Equation 6 by inverting to define a scattering angle, $\theta_{sampled}$, given a random number, $\xi' \in (0, 1)$, by,

$$\theta_{sampled} = \text{acos}(2\xi' - 1) \qquad \text{Eqn.8}$$

These two angles, $\theta_{sampled}$ and $\phi_{sampled}$, completely describe the photon direction in the Monte Carlo simulation.

A blackbody spectrum is used to describe the photon energy distribution [3]. However, the temperature of the radiator surface is location dependent. Hence, the photon birth location is first determined then a blackbody spectrum is constructed based on the local temperature. The photon production density, $n(E)$, that is emitted from a blackbody radiator at a temperature T_0 (K) with energy in dE about E is given by

$$n(E)dE = \frac{8\pi\varepsilon E^2}{(hc)^3}\frac{1}{e^{E/(kT_o)} - 1}dE \qquad \text{Eqn. 9}$$

where,

$hc = 1.240\text{x}10^3$ eVnm and
k = Boltzmann's constant.

In the Monte Carlo Ray-Tracing code, the source photon energies are sampled from the corresponding probability distribution based on

$$p(E)dE = \frac{\frac{8\pi E^2}{(hc)^3}\frac{1}{e^{E/(kT_o)} - 1}dE}{\int_0^{E_{max}} \frac{8\pi E^2}{(hc)^3}\frac{1}{e^{E/(kT_o)} - 1}dE} \qquad \text{Eqn. 10}$$

where E_{max} is set to an arbitrarily large value of $10kT_o$.

Photon Transport

Once the location, direction and energy of the source photons are determined, the Monte Carlo transport simulation can begin. Millions of photon histories are simulated in typical Monte Carlo calculations. Scattering events from the reflective walls and filters are common during a photon's life cycle. An accurate model of these scattering events is of paramount importance in a Monte Carlo calculation since these scattering events occur frequently. Figure 7 shows the computational model of the cavity experiment with some possible photon histories superimposed.

In the Monte Carlo Ray-Tracing code, materials are considered either opaque or transparent to these photons and every material interface is assigned a reflection probability. Surface reflectance values for the important materials have been obtained as a function of photon wavelength, polarization, and angle of incidence. The reflectance data for the materials used in the cavity experiments has been introduced into Monte Carlo in the form of boundary conditions. These boundary conditions are determined for individual photons each time a photon strikes a boundary. A photon of energy, E_γ, and polarization, ρ_γ, that hits a surface at an angle, θ_γ, that has an energy/angle/polarization dependent reflection probability, $P(E,\theta,\rho)$, is reflected if

$$\xi \le P(E_\gamma, \theta_\gamma, \rho_\gamma) \qquad \text{Eqn. 11}$$

where ξ = a random number $\in (0, 1)$. Otherwise, the photon enters the material where it is absorbed or transmitted depending on the material opacity. Hence, the accuracy of the Monte Carlo Ray-Tracing code results are strongly dependent upon the accuracy of the surface reflectivities and material opacities.

The code can be used to calculate the heat flux absorbed in any region of interest regardless of model geometry. Analytic solutions for the heat flux are generally only possible for simple geometries, *e.g.*, parallel and perpendicular rectangular plates or simple cavities. View factors and heat transfer between infinite parallel plates were calculated as part of the Monte Carlo validation procedure. Analytic view factors become very difficult to define for all, but the most simple geometries. The Monte Carlo Ray-Tracing code absorption edits are equivalent to view factors, by definition, and are calculated for any geometry of interest. Figure 8 shows the geometry for a view factor calculation for two parallel χ-by-χ square plates with a separation distance of Υ and the analytic solution [4] for the view factor is given by

$$F_{1\to 2} = \frac{2}{\pi\chi\Upsilon}\left[\ln\left(\frac{(1+\chi^2)(1+\Upsilon^2)}{1+\chi^2+\Upsilon^2}\right)^{1/2} + \chi\sqrt{1+\Upsilon^2}\,\text{atan}\frac{\chi}{\sqrt{1+\Upsilon^2}} + \Upsilon\sqrt{1+\chi^2}\,\text{atan}\frac{\Upsilon}{\sqrt{1+\chi^2}} + (-\chi)\,\text{atan}\chi + (-\Upsilon)\,\text{atan}\Upsilon\right]$$

Eqn. 12

The analytic solution for this geometry is $F_{1\to 2} = 0.589$ while Monte Carlo calculates the view factor to be $F_{1\to 2} = 0.590$. Other view factors were calculated as part of the validation with similar good agreement. In addition, a set of radiative heat transfer calculations between infinite parallel plates was performed and the results from the Monte Carlo Ray-Tracing code were in good agreement with the analytic solution. The Monte Carlo code only predicts the I_{sc} output of each cell or column of cells. Its data has to be post processed using a SABER circuit simulation to predict I_{sc} for the entire array. To calculate an overall efficiency, Eqn. 1, requires the open circuit voltage and fill factor. The Monte Carlo Ray-Tracing code does not calculate these parameters and was used primarily for absorbed heat flux predictions.

Discussion of Results

Results from both measurements and computational predictions were generated in the course of performing the cavity studies. In addition, absorbed heat fluxes and short circuit currents became the focus of both the measurements and the computational methods. As a first step in analyzing the results, heat flux calculations from the two computer codes were compared. Table 1 lists the results from the testing of various grey absorber materials using the infinite parallel plate geometry (graphite, gallium antimonide wafer and gold foil). There is good agreement (12% or less) between the predicted absorbed heat flux of TPVCalc and the Monte Carlo Ray-Tracing code. These results were not expected to be identical since the Monte Carlo code filter reflectivities are represented by 100 evenly spaced energy points while the TPVCalc solution is based on reflectivities of variable energy resolution. TPVCalc also assumes that all energy emitted from the radiator is incident upon the cell; whereas, the Monte Carlo Ray-Tracing code accounts for absorptions in materials other than the array and incorporates cavity end losses into its predictions. In this series of comparisons, the heat flux predictions from the TPVcalc and the Monte Carlo Ray-Tracing methods are in good agreement.

One of the goals of these cavity studies was to determine if the measured device efficiency could be predicted. Table 2 shows the data predicted and measured for a 16 cell array. For an average radiator temperature of 1090°C and cell temperature of 25°C, the array's efficiency was predicted to be approximately 7.0% using TPV-Calc based upon electrical characterization of the array. Testing of 16, 1 cm^2 TPV cells in a 4x4 configuration (array) resulted in an array efficiency of 6.3%. Although the relative absorbed heat flux and short circuit current measurements are higher than predictions, as will be discussed, the overall efficiency of the device is only affected slightly. This is due to the increase of both the numerator and denominator of equation 1. The measured efficiency of 6.3% is lower than the predicted efficiency of the infinite parallel plate model of 7.0%.

Significant differences were observed between the measured and calculated electrical current and heat fluxes. The absorbed heat flux of the array was predicted to be 6.32 W/cm^2 and 5.34 W/cm^2 using TPVCalc and Monte Carlo, respectively. The measurements show that 7.8 W/cm^2 were absorbed in the TPV array for a radiator and cell temperature of ~1090°C and ~25°C, respectively. In addition, measurements indicate that the array produced approximately 0.324 volts/row and 3.45 amps/row for a total 8.62 watts at a the same temperatures. Both computer codes predicted a short circuit current (I_{sc}) that is ~20% lower than the measured value. Hence, the computer codes under-predict both the heat flux and short circuit current when compared to measured values.

Analysis illustrates that an average radiator temperature of approximately 65°C higher than the measured temperature could account for both of these discrepancies. This disagreement could also be explained by low measurements in spectral quantum efficiency and errors in filter reflectivity. Modeling assumptions (the Monte Carlo Ray-Tracing code assumes purely specular reflectivity within the cavity) and/or radiator emissivity at temperature could also play a role in the observed discrepancies. The predicted absorbed heat flux is also strongly dependent on the radiator surface temperature distribution. An estimated 10% of this discrepancy may be attributable to the uncertainty in our calorimetry measurements as well.

Table 3 summarizes the various parameters in equation 2 and the effects of the various measured and calculated electrical and optical properties on array efficiency. This table also provides a comparison of efficiency between the measured 16 cell array and efficiency for a high performing 0.55 eV InGaAs cell. The data in this table suggests that array efficiency should approach 13.6% for an array constructed of cells with characteristics identical to that of the single cell under uniform illumination. This assumes that the higher than predicted heat flux and short circuit current are both caused by a photon flux which does not agree with measured radiator temperature.

Conclusions

In conclusion, two computer codes (TPVCalc and a Monte Carlo Ray-Tracing code) were developed to predict 16 cell array efficiency in a cavity geometry. The results obtained from these codes agreed well with analytic solutions for various, simple problems. The codes were also in good agreement with the absorbed heat flux measurements of known grey absorbers. TPVCalc was used to predict the efficiency of the array used in this initial test to be ~7.0%. Actual measurements of the array's efficiency was ~6.3%, showing good agreement with the codes predictions. However, the code predicted significantly lower absorbed heat flux and short circuit current from the array. The Monte Carlo Ray-Tracing code was used to calculate a best estimate of the heat flux using the exact geometry. The heat absorbed calculated in the Monte Carlo Ray-Tracing code was similar to that of the TPVCalc results. This adds credibility to the calculated heat flux over the measured heat flux values given the modeling input.

Efficiency was not significantly affected by this discrepancy because the two measurements were ratioed to quantify efficiency. Possible reasons for this discrepancy include inaccurate radiator temperature measurements and other modeling inputs. The array used in this testing was comprised of poor performing cells and was purposely selected for this testing. Use of better cells and in this type of array configuration a more uniform radiator would result in efficiencies considerably higher (~13.6%). Table 3 shows the improvements in cell, spectral control and manufac-

turing required to improve array efficiency from 6.3% to approach that of the aforementioned prediction.

References

1) Charache, G. W. et. al., "Measurement of Conversion Efficiency of Thermophotovoltaic Devices", Proc. of the 2nd NREL Conf. on TPV Gen. of Elec., 351 (1995).

2) Baldasaro, P. F. et. al., "Experimental Assessment of Low Temperature Voltaic Energy Conversion", Proc. of the 1st NREL Conf. on TPV Gen. of Elec., 29 (1994).

3) Krane, Kenneth, *Modern Physics*, John Wiley & Sons, New York, 1983.

4) Modest, M.A., Radiative Heat Transfer, McGraw-Hill, New York, 1993.

5) OptiLayer Code Ver. 3.06, Debell Design, Los Altos, CA, 1996.

Acknowledgments

The authors would like to acknowledge Dr. J. L. Egley, Dr. L. R. Danielson, Dr. J. R. Parrington and E. J. Brown for testing and analysis support. We would also like to thank Dr. G. W. Charache, and Dr. S. R. Sreepada for their valuable insight and suggestions.

Table 1: Predicted heat flux comparisons for various greybody absorbers

	Radiator Temperature (°C)	*TPVCalc Heat Flux (W/cm^2)	**Monte Carlo Heat Flux (W/cm^2)	% Difference
Graphite	1055	14.4	14.3	0.9
GaSb Wafer	1055	10.31	10.30	0.1
Gold Foil	1096	0.34	0.30	11.7

*Predictions based on average edge radiator temperature
**Predictions based on parabolic radiator temperature distribution

Table 2: 16 cell array predictions and measurements

	Radiator Temperature (°C)	Absorbed Heat Flux (W/cm^2)	Short Circuit Current (A)	Power out (W)	Efficiency (%)
*TPVCalc	1108	6.32	11.8	8.79	7.0
**Monte Carlo	1109	5.345	12.0	NA	NA
Measurement	1108	7.9	13.88	8.62	6.3

*Predictions based on average edge radiator temperature
**Predictions based on parabolic radiator temperature distribution

Table 3: Differences between single cell and array efficiency measurements

F_o	V_{oc}/E_g	FF	QE_{int}	F_u cell	F_u module	$F_{unknown}$	η	Suspected Causes
0.80	0.63	0.68	0.68	0.60	1.0	1.0	14.0	Measured single cell η @ 1090°C
0.80	0.63	0.68	**0.66**	0.60	1.0	1.0	13.6	Low QE
0.80	**0.62**	**0.67**	0.66	0.60	1.0	1.0	13.2	High measured dark current
0.80	**0.58**	0.67	0.66	0.60	1.0	1.0	12.3	Lower array ideality factor
0.80	0.58	0.67	0.66	**0.55**	1.0	1.0	11.3	Higher Reflection of above bandgap photons
0.80	0.58	0.67	0.66	0.55	**0.90**	1.0	10.2	TPV cell inactive area and cracks
0.80	0.58	**0.52**	0.66	0.55	0.90	1.0	7.9	25 milliohm R_s measured for array
0.80	0.58	0.52	**0.65**	0.55	**0.88**	1.0	7.6	Angle of incidence effects in cavity
0.80	0.58	**0.48**	0.65	0.55	0.88	1.0	7.0	Measured array fill factor
0.80	0.58	0.48	0.65	0.55	0.88	**0.90**	6.3	Measured array efficiency

*Bold values indicate the parameter that has been affected by the suspected cause

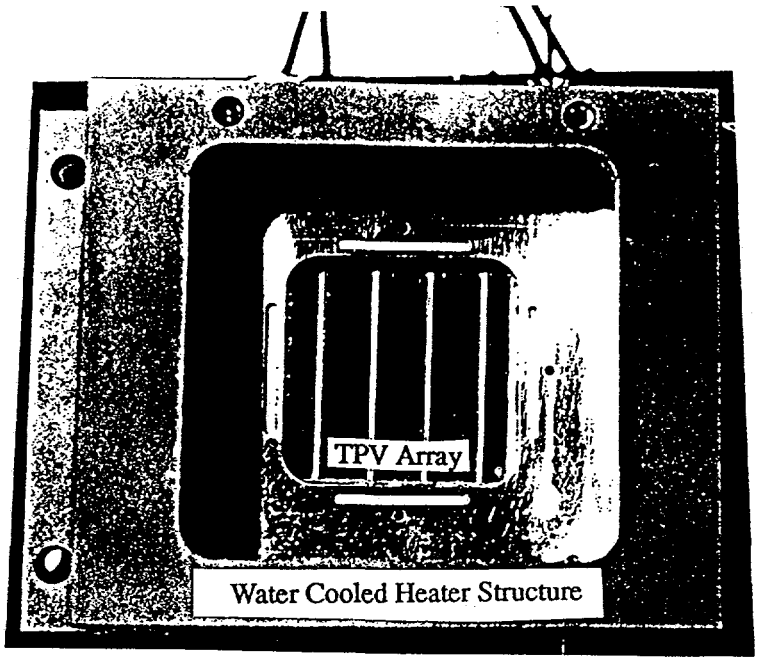

Figure 1. Top view of the heater cavity with the radiator material removed, showing the window for the 16 cell array.

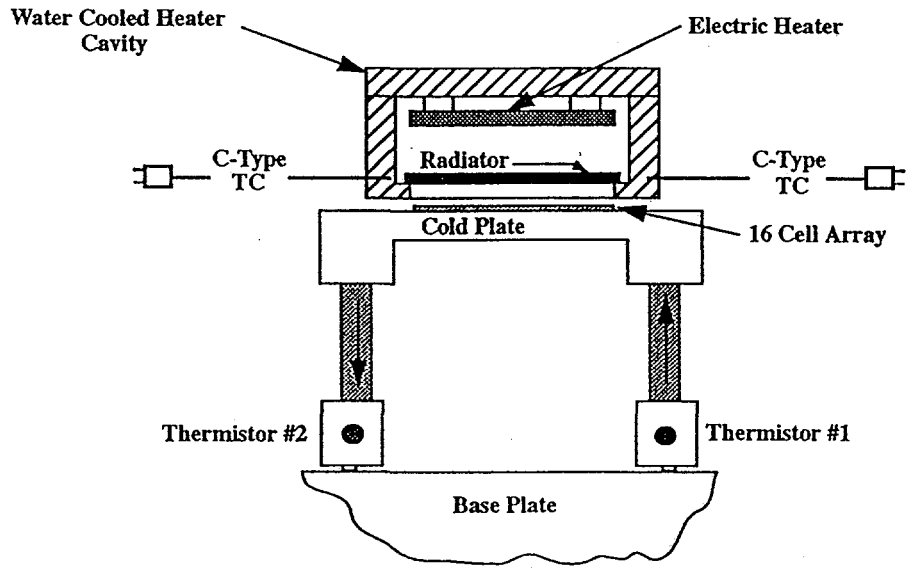

Figure 2. Schematic representation of the heater cavity test stand.

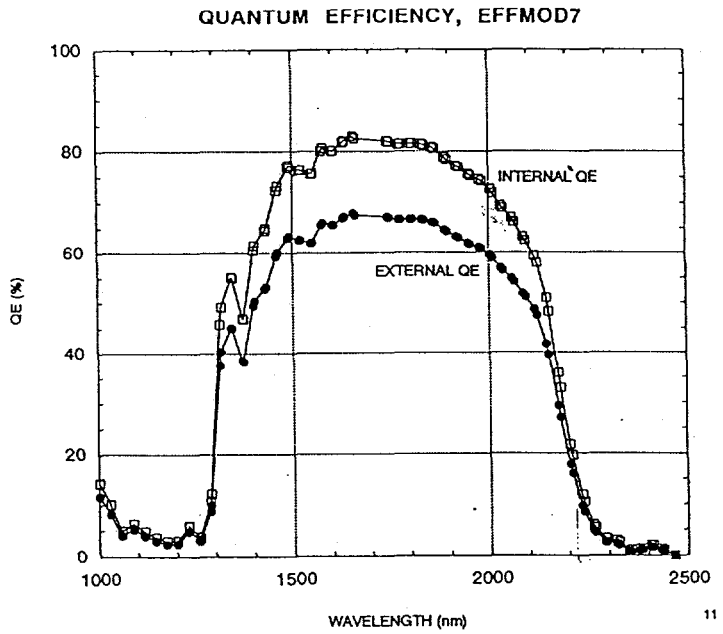

Figure 3: Internal and external quantum efficiency of a typical cell on the sixteen cell array tested in the efficiency test.

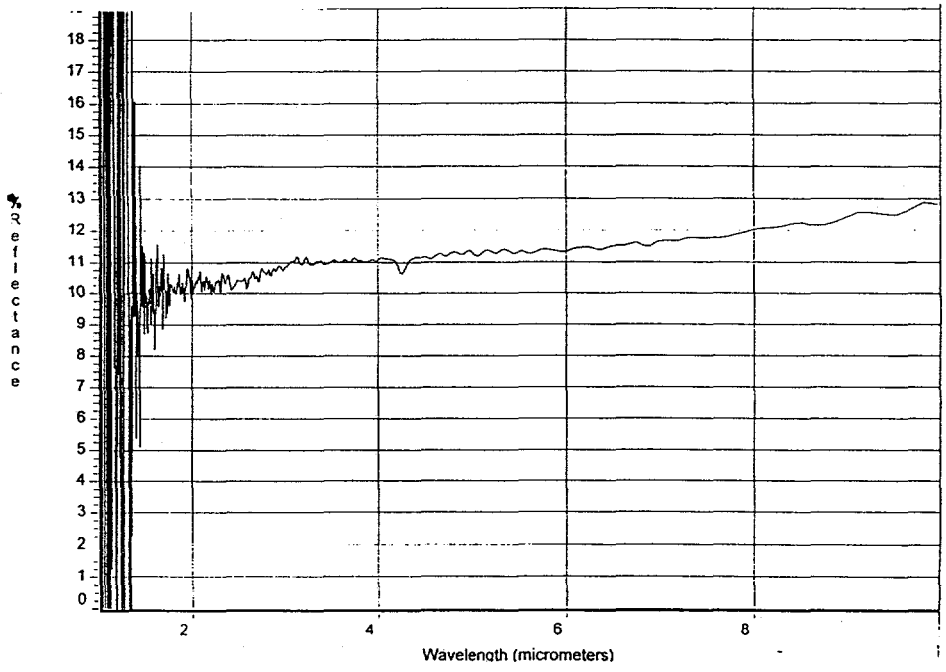

Figure 4: Measured reflectivity of the Poco Graphite radiator used in the efficiency test. The measured data was taken with an integrating sphere/FTIR at room temperature.

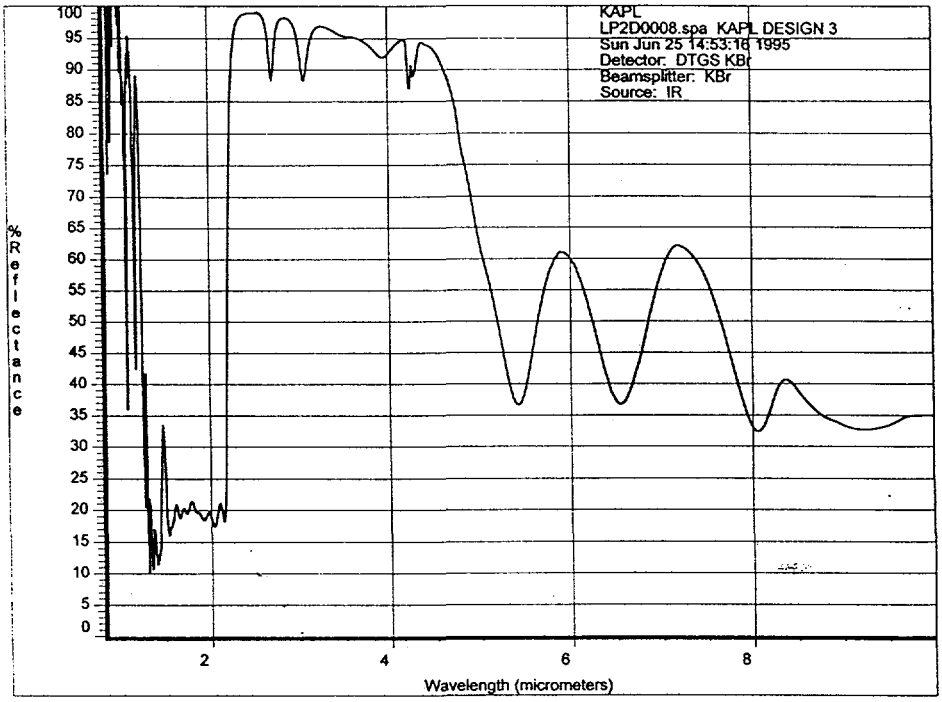

Figure 5: Typical spectral reflection characteristics of an interference filter for the array used in the efficiency test. The measurement was taken using an FTIR spectrometer.

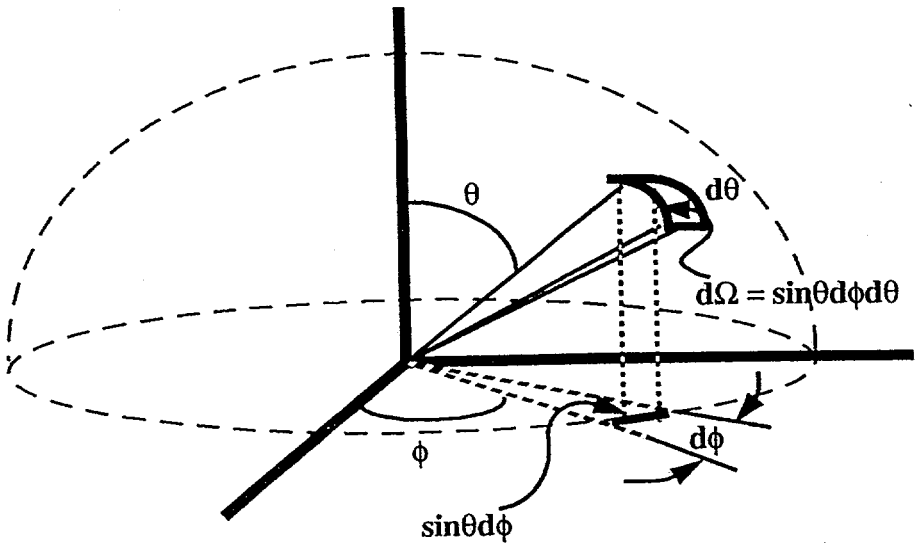

Figure 6. Solid angle integration.

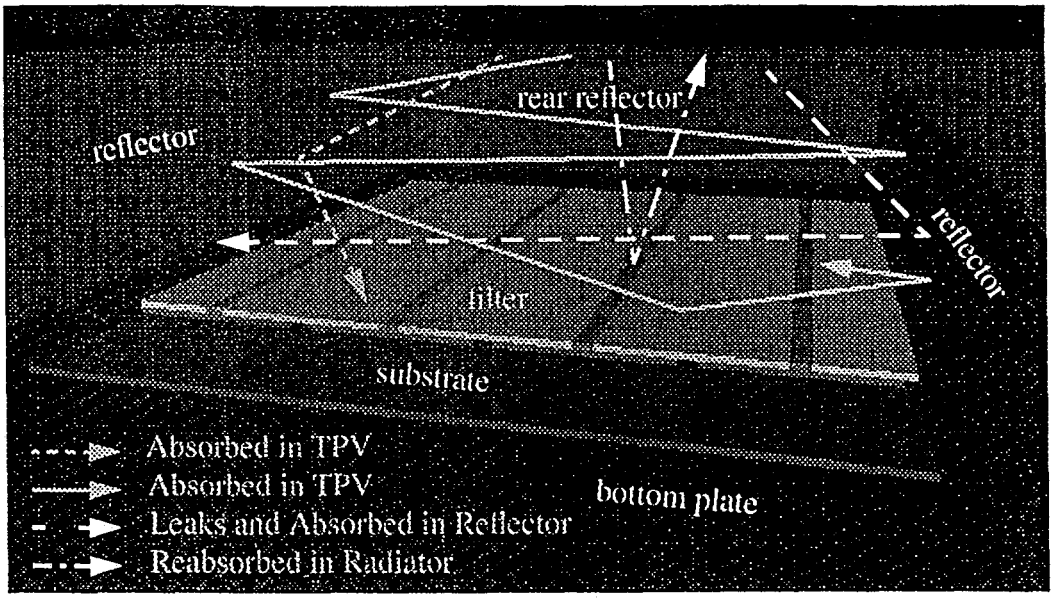

Figure 7. Possible photon paths in the cavity, front reflector and radiator are shown in this view.

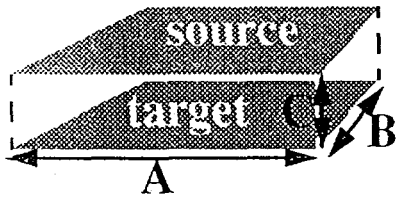

where,
A = 1.62 in.,
B = 1.61 in.,
C = 0.47 in.,
$\chi = (A/C)$ and
$\Upsilon = B/C$

Figure 8: Geometry for the view factor calculation